

# Deterministic measurement of the Purcell factor in microcavities through Raman emission

X. Checoury,\* Z. Han, M. El Kurdi, and P. Boucaud

*Institut d'Électronique Fondamentale, CNRS Univ Paris Sud 11, Bâtiment 220, F-91405 Orsay Cedex, France*

(Received 21 December 2009; published 18 March 2010)

We show that a deterministic value and measurement of the Purcell factor in a semiconductor microcavity can be obtained by using spontaneous Raman scattering as an internal source. In this case the emitter characteristics are entirely determined by the cavity design and do not depend on uncontrolled random factors, as it is usually the case when quantum dot emitters are used. We derive a theoretical expression for the Purcell factor of the cavity in the particular case of Raman scattering, in very good agreement with the experimental measurement.

DOI: [10.1103/PhysRevA.81.033832](https://doi.org/10.1103/PhysRevA.81.033832)

PACS number(s): 42.50.Pq, 78.30.Am, 42.70.Qs

## I. INTRODUCTION

Recently, optical microcavities having dimensions comparable to the light wavelength have gained a considerable interest for their ability to control and manipulate the spontaneous emission [1–4]. In such cavities, the enhancement of the spontaneous emission rate in the weak coupling regime through the Purcell effect [5] can lead to the realization of wide-bandwidth thresholdless microlasers or highly efficient single-photon sources. The observation and the precise knowledge of the maximum rate enhancement given by the Purcell factor remain usually limited by the characteristics of the quantum dot emitters commonly embedded in these structures. The dipole orientation, the spatial location, and the spectral matching of the quantum dots with the cavity modes are not always precisely known. Moreover, at room temperature, the broad homogeneous linewidth emission spectra of these emitters limits the achievable rate enhancement. In contrast, spontaneous Raman scattering is universally present in solids, exists for any frequency of incident light and, as a consequence, can be used as an internal source to probe microcavities. Similarly to other scattering processes [6,7], Raman scattering rate can be enhanced by engineering the optical density of states [8–10].

## II. THEORY OF THE PURCELL ENHANCEMENT OF RAMAN SCATTERING

If we consider the spontaneous Raman scattering rate in a bulk semiconductor for a given pump polarization and orientation,  $\tau_R^{-1}$ , the emission rate in a particular cavity mode can be written as  $F_R \tau_R^{-1}$ , where  $F_R$  is the Purcell enhancement factor for the Raman scattering emission. The mean number of Stokes photon  $N_s$  generated in a cavity by the Raman scattering of  $N_p$  pump photons is given by the following rate equations [11]:

$$\frac{dN_s}{dt} = -\frac{N_s}{\tau_s} + F_R \frac{N_p}{\tau_R} + GN_p N_s \quad (1)$$

$$\frac{dN_p}{dt} = -\frac{N_p}{\tau_p} - (F_R + \gamma) \frac{N_p}{\tau_R} - GN_p N_s + \kappa_{in} P_p, \quad (2)$$

where  $\tau_{s(p)}$  are the Stokes (pump) photon lifetime in the resonator,  $G$  is the gain due to stimulated Raman scattering,  $\kappa_{in}$

a constant relating the pump photon number injected by time unit in the cavity to the incident pump power  $P_p$ , and  $\gamma \tau_R^{-1}$  is the spontaneous emission rate in every other mode including the continuum modes. These equations are formally similar to those used for more classical semiconductor microcavity lasers if  $\tau_p$  is interpreted as the nonradiative lifetime and  $\tau_R$  as the radiative lifetime [12]. Because the spontaneous Raman scattering is a rather weak process in semiconductor,  $\tau_R$  is of the order of 10  $\mu$ s as compared to  $\tau_p$  that can be as low as a few picoseconds. As a consequence, it appears from these equations that the equivalent semiconductor microcavity structure would be dominated by the “non-radiative”-like rate  $\tau_p$  rather than by the radiative rate  $(F_R + \gamma) \tau_R^{-1}$  that is usually measured to characterize the Purcell effect. However, despite the small efficiency of the spontaneous emission, the value of  $F_R$  can be measured accurately from the collected Stokes power directly. In steady state, the dependence of the Stokes photon number with the input pump power is deduced from Eqs. (1) and (2) by  $\kappa_{in} P_p = \tau_s^{-1} F_R^{-1} [N_s / (N_s + 1)] [F_R N_s + (F_R + \gamma) + \tau_R / \tau_p]$  where we used the fact that the spontaneous rate is equal to the stimulated rate induced by one Stokes photon in the cavity, i.e.,  $F_R / \tau_R = G$ . Below laser threshold,  $N_s \ll 1$  and  $F_R$  can be obtained from the collected Stokes power  $P_s^{\text{coll}}$ ,

$$F_R = \frac{\tau_R \kappa_{out} P_s^{\text{coll}}}{\tau_p \kappa_{in} P_p} \quad (3)$$

with  $\kappa_{out}$  a coupling constant relating the Stokes photon number escaping from the cavity by unit time,  $N_s / \tau_s$ , to  $P_s^{\text{coll}}$ . As will be seen below, all the quantities involved in this expression can be obtained from optical measurements and the above expression provides a direct method for measuring  $F_R$ .

A theoretical expression of the Purcell factor,  $F_R$ , involving the characteristic parameters of the cavity only, can also be derived in the case of Raman scattering. Here, we consider, as in the experiments, silicon microcavities with pump light polarized along the [110] crystallographic direction. In silicon, the Raman effect has a symmetric and relatively narrow linewidth of 105 GHz, much narrower than the one of semiconductor quantum dots at room temperature. Moreover, around a wavelength of 1.5  $\mu$ m and at low power, the absence of absorption in silicon allows the precise measurement of the optical cavity parameters like the quality factor while the volume and location of the active medium can be controlled by the pump laser beam. As shown in

\*xavier.checoury@ief.u-psud.fr

the appendix, an electromagnetic treatment of the stimulated Raman scattering tuned at the cavity resonance gives  $G = 2\Gamma_r / (2\Gamma_r + \Gamma_s) g_R^B hc^3 / (n_p n_s V_R \lambda_p)$  where  $n_s, n_p$  are the refractive index of silicon at the Stokes and pump wavelength  $\lambda_s, \lambda_p$  respectively.  $\Gamma_r / \pi = 105$  GHz is the full width at half maximum (FWHM) at room temperature [13] of the Raman scattering and  $\Gamma_s = \tau_s^{-1}$ . The bulk Raman gain coefficient, in units of  $\text{m W}^{-1}$ , is noted  $g_R^B$  and  $V_R$  is the Raman modal volume of the cavity. A similar calculation relates the spontaneous rate in the bulk  $\tau_R^{-1}$  for a [110] polarized excitation to the Raman gain in the bulk  $g_R^B$ :  $\tau_R^{-1} = 4\pi g_R^B hc^2 n_s^2 (2\Gamma_r) / (3n_p \lambda_p \lambda_s^2)$ . As a consequence, the Purcell factor in the case of Raman scattering is given by:

$$F_R = G\tau_R = \frac{3}{8\pi^2 V_R} \frac{Q_r Q_s}{Q_r + Q_s} \left(\frac{\lambda_s}{n_s}\right)^3, \quad (4)$$

where the quality factors are given by  $Q_s = 2\pi c \tau_s / \lambda_s$  and  $Q_r = \pi c / (\Gamma_r \lambda_s)$ . Equation (4) gives the spontaneous rate enhancement of Raman scattering for a cavity tuned to the Raman resonance for a pump polarization oriented along the [110] crystallographic axis. Because the Raman emission into the bulk occurs along two orthogonal polarizations, this formula differs from the Purcell's one by a factor two in the denominator. The spectral overlap between the cavity resonance and the Raman emission is taken into account by the harmonic mean of the  $Q$  factors while the spatial overlap between the field and the emitter, that is not a single localized dipole in the cavity, is included in the Raman volume. The Raman volume consequently differs from the Stokes mode volume and is given by

$$V_R = \frac{\int \varepsilon_s(\mathbf{r}) |\mathbf{e}_s(\mathbf{r})|^2 d^3r \int \varepsilon_p(\mathbf{r}) |\mathbf{e}_p(\mathbf{r})|^2 d^3r}{n_p^2 n_s^2 \int_{\text{Si}} \mathbf{e}_s^*(\mathbf{r}) \xi_{ijkl}^{(3)} \mathbf{e}_p(\mathbf{r}) \mathbf{e}_p^*(\mathbf{r}) \mathbf{e}_s(\mathbf{r}) d^3r}, \quad (5)$$

where  $\varepsilon_{s(p)}$  is the relative permittivity,  $\mathbf{e}_{s(p)}(\mathbf{r})$  is the Stokes (pump) cavity eigenmode spatial part, and the integral of the denominator is on the silicon volume only. Because all the nonzero components of the Raman susceptibility tensor  $\chi_{ijkl}^{(3)}$  have the same magnitude in silicon, we have noted  $\xi_{ijkl}^{(3)}$ , the tensor the components of which equal 0 if the corresponding components of  $\chi_{ijkl}^{(3)}$  are zero and 1 otherwise.

### III. EXPERIMENTAL SETUP AND RESULTS

The studied cavities are made by a 24- $\mu\text{m}$ -long photonic crystal (PC) W1 waveguide oriented along the  $[\bar{1}\bar{1}0]$  direction of a silicon-on-insulator (SOI) wafer with a 200-nm-thick Si layer on a 2- $\mu\text{m}$ -thick oxide layer which was removed after the processing of the structures [14]. The suspended W1 waveguides were classically fabricated in triangular lattice patterns by omitting to drill one row of holes along the  $\Gamma\text{K}$  direction. The designed photonic crystals have a lattice period  $a$  of 454 nm and an air hole radius equal to  $0.26a$ . To improve light injection and collection, light was injected into the W1 with a lensed fiber through two suspended ridge waveguides terminated at their ends by inverted tapers.

Figure 1 shows the transmission spectra of a 24- $\mu\text{m}$ -long W1 waveguide with its two access waveguides near the W1 cut-off wavelength. Because of the mode mismatch between the W1 and the access waveguide at these frequencies, the W1

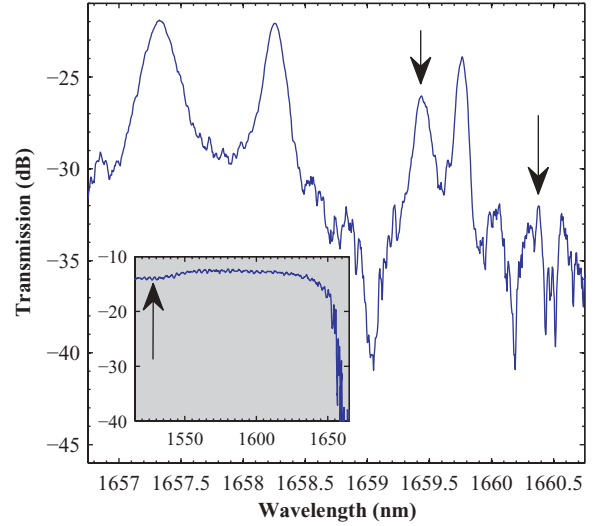


FIG. 1. (Color online) Transmission spectrum of a PC W1 waveguide with its access waveguides near the W1 cut-off wavelength (OSA resolution 0.1 nm). The two arrows indicate the wavelengths of the studied modes. Inset: overview of the W1 transmission (OSA resolution 0.5 nm). The arrow indicates the pump wavelength.

waveguide behaves like a Fabry-Perot cavity whose resonant modes are clearly seen. The measured quality factor of the resonance at 1659.4 nm is  $10^4$ . The quality factor of the two last hardly visible resonances at 1660.4 nm and 1660.6 nm have the same value of  $4.5 \times 10^4$ . The inset shows an enlarged view of the transmission spectrum. As expected, in the frequency range of PC high group velocity, the PC waveguide is well matched with the access waveguide. Indeed, below the light line, i.e., for wavelengths longer than 1540 nm, and in the high-speed velocity frequency range of the W1, the insertion losses of the whole sample are similar to those of the access waveguide alone. The W1 propagation losses are measured to be around 58 dB/mm at the wavelength of the pump, i.e., for wavelengths shorter than 1540 nm.

To observe the Raman scattering, a continuous tunable laser source and an erbium-doped fiber amplifier are used. We first measure the Raman scattering generated in the output ridge access waveguide. To do so, we choose a pump wavelength of 1532 nm and measure the spontaneous Raman scattering near 1665 nm, i.e., in the stop band of the W1 waveguide. Since at this wavelength the Raman scattering generated in the input ridge waveguide is blocked by the W1 and no scattering occurs in the PC waveguide, we only collect the Raman scattering generated in the output suspended waveguide. The result is displayed in the inset of Fig. 2. For a pump power of 6.7 mW coupled in the output suspended waveguide, the collected Stokes power is 1.1 pW. The FWHM of the spontaneous Raman scattering generated in the access waveguide is, as expected, equal to  $\sim 105$  GHz and reflects the phonon lifetime in silicon. The situation differs drastically for the spontaneous Raman scattering generated in the 24- $\mu\text{m}$ -long W1 waveguide for a pump wavelength of 1527.7 nm [Fig. 2(a)]. The Raman scattering has its spectrum strongly reshaped by the photonic crystal waveguide since the FWHM of the different peaks is below 0.2 nm, the optical spectrum analyzer (OSA) resolution. Moreover, the Raman spectra at high pump power reveal

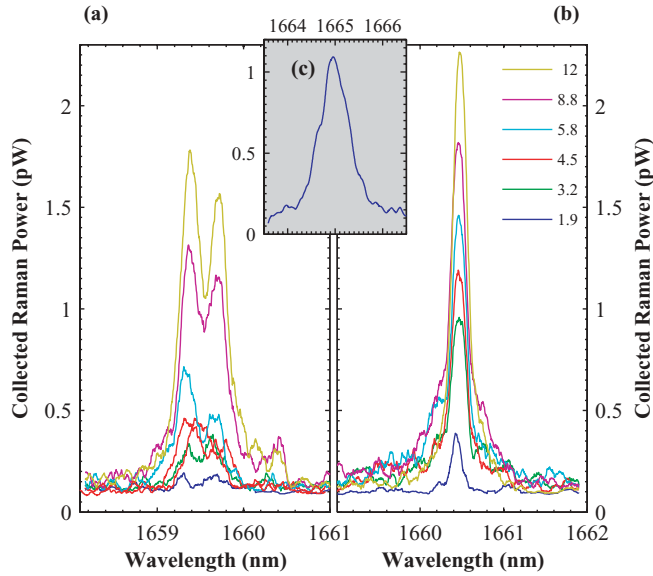


FIG. 2. (Color online) Raman emission spectra measured for pump wavelength of 1527.7 nm (a) and 1528.3 (b) corresponding to spontaneous Raman spectra centered at 1659.6 and 1660.4 nm, respectively (OSA resolution 0.2 nm). The pump powers at the input of the W1 waveguide are varied in the 1.9- to 12-mW range. (c) Raman scattering generated in the output access waveguide alone for a pump power of 12 mW at the entrance of the W1 waveguide corresponding to 6.7 mW in the access waveguide due to the W1 losses. The legend gives the curves shown from top to bottom in the figure.

a resonance at 1660.4 nm [Fig. 2(b)] that is hardly visible on the transmission spectra of Fig. 1. Changing the pump wavelength from 1527.7 to 1528.3 nm allows us to generate Raman scattering in a single narrow mode.

No stimulated Raman scattering occurs [15,16] since, as seen in Fig. 3, the dependence of the Raman power generated inside the W1 waveguide is linear with the pump power for the 1659.4- and 1660.4-nm resonances. In Fig. 3, the collected power has been corrected by subtracting the Raman power generated inside the access guide and taking into account the propagation losses as well as the coupling losses at the inverted taper tip.

The Stokes photon number in the cavity is related to the power escaping from the cavity by  $P_s = N_s \hbar \omega_s / \tau_s$ . However, only a fraction of this power,  $P_s^{\text{coll}} = N_s \hbar \omega_s / \tau_s^{\text{coll}}$ , is indeed collected in the access waveguides. If we assimilate the W1 waveguide to a symmetric Fabry-Perot resonator, the transmission peaks  $T_{\text{max}}$  are equal to the ratio  $(\tau_s / \tau_s^{\text{coll}})^2$ . Hence, we can deduce from the measurements the value of the collected power as a function of the Stokes photon number:  $P_s^{\text{coll}} = \kappa_{\text{out}}^{-1} N_s / \tau_s = 1/2 \sqrt{T_{\text{max}}} N_s \hbar \omega_s / \tau_s$ , where the 1/2 factor indicates that we collected the power emitted at only one end of the cavity. From the transmission of the W1 waveguide at the wavelengths 1659.4 and 1660.4 nm shown in Fig. 1, we respectively get  $T_{\text{max}} \approx -15$  dB and  $P_s^{\text{coll}} = 9.3$  pW as well as  $T_{\text{max}} \approx -21$  dB and  $P_s^{\text{coll}} = 6.8$  pW for a pump power of 10 mW inside the 24- $\mu\text{m}$ -long photonic crystal. Similarly for the pump,  $T_{\text{max}} \approx 1$  and we find  $\kappa_{\text{in}} P_{\text{in}} = (\hbar \omega_p \sqrt{T_{\text{max}}})^{-1} P_{\text{in}} \approx 1.3 \times 10^{-21} \text{ s}^{-1}$ , and  $\tau_p = 0.26$  ps considering a group index

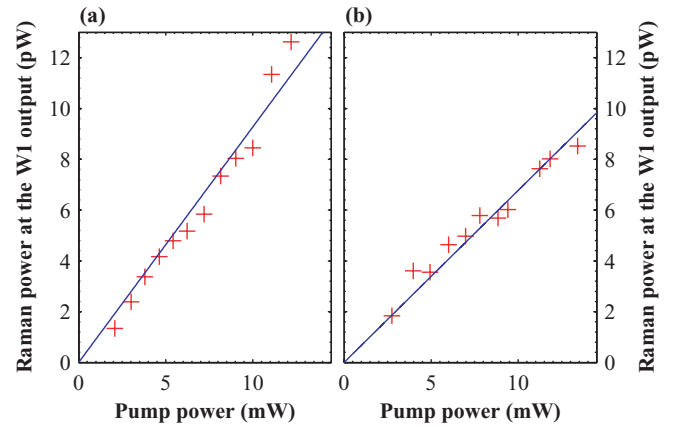


FIG. 3. (Color online) Raman power generated inside the W1 waveguide. The power coupled to the output access waveguide at 1659.4 nm (a) and at 1660.4 nm (b) is represented as a function of the pump power at the input of the W1 waveguide. The pump wavelengths are 1527.5 and 1528.3 nm, respectively. The power is integrated over a 0.5-nm bandwidth and the lines are a least-squares linear fit of the data.

$n_p^g$  of 4.4 and propagation losses of 58 dB/mm for the pump at  $\lambda_p = 1527.5$  nm and  $\lambda_p = 1528.3$  nm. A value of the Raman gain for silicon commonly reported in the literature is between 20 and 76 cm/GW. For a Raman gain of 57 cm/GW [17],  $\tau_B = 13 \mu\text{s}$  and we deduce the respective experimental factors  $F_R$  0.56 and 0.82 from Eq. (3) for the resonant modes at 1659.4 and 1660.4 nm. Using the same value of the Raman volume for the two modes,  $V_R = 7.9 \times 10^{-18} \text{ m}^3$ , computed from three-dimensional plane wave simulations, theoretical Purcell factors calculated with Eq. (4) are  $F_R \approx 0.8$  and  $F_R \approx 0.9$  in very close agreement with the experimental values. This agreement could be even better if we consider a slightly reduced value of the Raman gain. This result shows the validity of our approach to deterministically measure the Purcell factor since its determination relies on easily measurable quantities only determined by the cavity design. This is in striking contrast with the quantum dot approach where spectral and spatial matching are usually unknown. If we suppose that the emission rate in the continuum of non resonant modes  $\gamma$  is not affected by the PC and thus remains near 1, the total rate of spontaneous emission is thus enhanced by a factor  $F + \gamma \approx 1.8$  as compared to the rate in the bulk. A Raman laser build on this cavity will be characterized by a spontaneous emission factor at room temperature  $\beta = F_R / (F_R + \gamma) = 0.44$  and above if we take into account that the emission in the continuum of radiation modes can be inhibited by the PC [18]. In our experiment, the Purcell factor is limited by the Raman volume 70 times larger than the typical small mode volume of ultimate PC cavities. Reducing the size of the cavity and as a consequence the Raman volume by a factor 20 while maintaining a  $Q$  factor around  $1.0 \times 10^4$  would then lead to a Purcell factor around 16, limited by the Raman gain linewidth. The  $\beta$  factor would then be at least equal to 0.94 and such a laser would exhibit remarkable properties in terms of high speed modulation.

#### IV. CONCLUSION

In conclusion, we have measured the Purcell factor for Raman scattering in silicon PC cavities at room temperature under continuous excitation. We have shown that the main difference in the expression of the Purcell factor between the standard case and the Raman scattering one is the use of the Raman volume that intrinsically takes into account the orientation, the spatial and spectral matching of the emitter. As a result, the emitted optical power is fully controlled and determined by the cavity design and by the pump beam. Since all the quantities involved are measurable, a very good agreement has been found with the experiment thus demonstrating the deterministic nature of the Purcell enhancement for Raman scattering. The observation of enhanced Raman scattering in cavities opens the route to the development of high  $\beta$  factor ultracompact lasers in silicon at room temperature.

#### APPENDIX: DERIVATION OF THE PURCELL FACTOR

To calculate the Purcell factor in a cavity, we start with the coupled-mode theory of the Raman effect [19,20]. We consider the slowly varying envelopes  $a_s(t)$  of the Stokes cavity mode  $\mathbf{E}_s(\mathbf{r}, t) = (a_s(t)\mathbf{e}_s(\mathbf{r})/A_s)\exp(-i\omega_s t)$ , where  $\mathbf{e}_s(\mathbf{r})$  is the cavity eigenmode spatial part and  $A_s^2 = 1/2 \int \varepsilon_0 \varepsilon_s(\mathbf{r}) |\mathbf{e}_s(\mathbf{r})|^2 d^3r$  a normalizing constant. The quantities  $a_p$ ,  $\mathbf{E}_p$ ,  $\mathbf{e}_p$ , and  $A_p$  are defined similarly for the pump mode. Replacing these expressions of  $\mathbf{E}_{s(p)}$  in the coupled Maxwell equations with the nonlinear polarization induced by the stimulated Raman effect  $\mathbf{P}_s^{\text{NL}} = \varepsilon_0 \chi_{ijkl}^{(3)}(\omega_s) \mathbf{E}_p \mathbf{E}_p^* \mathbf{E}_s$ , we get the equation verified by the slowly varying envelopes  $a_s(t)$ :  $da_s/dt = -a_s/2\tau_s + g_R |a_p|^2 a_s$ , where we have neglected  $d^2 a_s/dt^2$  in front of  $\omega da_s/dt$ . The Raman gain in the cavity  $g_R$ , in units of  $\text{J}^{-1} \text{s}^{-1}$ , is given by  $g_R = i\omega_s \varepsilon_0 \int \mathbf{e}_s^*(\mathbf{r}) \chi_{ijkl}^{(3)} \mathbf{e}_p(\mathbf{r}) \mathbf{e}_p^*(\mathbf{r}) \mathbf{e}_s(\mathbf{r}) d^3r / (4A_s^2 A_p^2)$ . Because all the nonzero components of the susceptibility tensor  $\chi_{ijkl}^{(3)}$  have the same magnitude, we can rewrite  $\chi_{ijkl}^{(3)}(\omega_p - \omega_s) = \chi_R^{(3)}(\omega_p - \omega_s) \xi_{ijkl}^{(3)}$  with  $\xi_{ijkl}^{(3)} = \chi_{ijkl}^{(3)} / \chi_{1221}^{(3)}$

and  $\chi_R^{(3)}(\Omega) = \chi_R^{(3)}(\Omega_R)(-2i\Gamma_r \Omega_R) / (\Omega_R^2 - \Omega^2 - 2i\Gamma_r \Omega)$ ,  $\Omega_R/2\pi = 15.6$  THz being the Raman shift and  $\Gamma_r/\pi = 105$  GHz being the FWHM [13]. The gain in the cavity can then be written as  $g_R(\Omega) = -\omega_s \text{Im}(\chi_R^{(3)}(\Omega)) / (\varepsilon_0 n_p^2 n_s^2 V_R)$  with the Raman volume given by Eq. (5). The maximum Raman gain in the cavity  $g_R(\Omega_R)$  is related to the more traditional bulk gain coefficient  $g_R^B$  in units of  $\text{m W}^{-1}$  by  $g_R(\Omega_R) = g_R^B c^2 / (2n_p n_s V_R)$ .

To study the spontaneous Raman scattering, it is convenient to introduce the mean Stokes (pump) photon number in the cavity  $N_{s(p)} = |a_{s(p)}|^2 / \hbar \omega_{s(p)}$  for the particular eigenmode considered. Multiplying the  $a_s$  rate equation by  $a_s^*$ , we get  $dN_s/dt = -N_s/\tau_s + 2g_R(\Omega) N_p \hbar \omega_p (N_s + 1)$ , where we have added one supplementary Stokes photon to take into account the spontaneous emission. Deriving these equations, we have supposed that the cavity frequency is tuned to the maximum Raman gain and that the linewidth of the cavity mode is much smaller than the one of the Raman spectrum. To take into account the linewidth of the cavity, the expression for the total number of photons spontaneously emitted is obtained by multiplying  $g_R(\omega_p - \omega_s) \approx g_R(\Omega_R) \Gamma_r^2 / [(\omega_p - \omega_s - \Omega_R)^2 + \Gamma_r^2]$  with the normalized Lorentzian spectral lineshape of the cavity mode  $(\Gamma_s/2\pi) / [(\omega_p - \omega_s - \Omega_R)^2 + (\Gamma_s/2)^2]$  where  $\Gamma_s = \omega_s/Q_s$  and by integrating the result. We obtain the spontaneous emission rate per pump photon in the cavity,  $G = 2\Gamma_r / (2\Gamma_r + \Gamma_c) 2g_R(\Omega_R) \hbar \omega_p$  for a cavity mode tuned at the maximum of Raman gain. To calculate the spontaneous emission rate in bulk silicon, we apply the formalism described above to a large cavity of volume  $V$  in silicon and get the number of scattered pump photon by time unit:  $dN_p/dt = -g_R^B c^2 \hbar \omega_p M b N_p / (n_p n_s)$ , where  $M = V \omega_s^2 (\pi \Gamma_r) n_s^3 / (\pi^2 c^3)$  is the total number of modes into which the system can radiate and  $b$  is a geometrical factor that accounts for the angular distribution of the scattered radiation [11]. Explicitly,  $b$  is equal to the average of the inverse Raman volume over all the Stokes modes. For a pump mode polarization aligned along the [110] crystallographic axis as in our experiment, we get  $b = 2/(3V)$ . The spontaneous emission rate in the bulk is thus given by  $\tau_R^{-1} = 4\pi g_R^B \hbar c^2 n_s^2 (2\Gamma_r) / (3n_p \lambda_p \lambda_s^2)$ .

- 
- [1] J. M. Gérard, B. Sermage, B. Gayral, B. Legrand, E. Costard, and V. Thierry-Mieg, *Phys. Rev. Lett.* **81**, 1110 (1998).
- [2] A. Kiraz, P. Michler, C. Becher, B. Gayral, A. Imamoglu, L. Zhang, E. Hu, W. V. Schoenfeld, and P. M. Petroff, *Appl. Phys. Lett.* **78**, 3932 (2001).
- [3] A. Badolato, K. Hennessy, M. Atature, J. Dreiser, E. Hu, P. M. Petroff, and A. Imamoglu, *Science* **308**, 1158 (2005).
- [4] D. Englund, D. Fattal, E. Waks, G. Solomon, B. Zhang, T. Nakaoka, Y. Arakawa, Y. Yamamoto, and J. Vučković, *Phys. Rev. Lett.* **95**, 013904 (2005).
- [5] E. Purcell, *Phys. Rev.* **69**, 681 (1946).
- [6] A. Mazzei, S. Götzinger, L. de S. Menezes, G. Zumofen, O. Benson, and V. Sandoghdar, *Phys. Rev. Lett.* **99**, 173603 (2007).
- [7] T. J. Kippenberg, A. L. Tchebotareva, J. Kalkman, A. Polman, and K. J. Vahala, *Phys. Rev. Lett.* **103**, 027406 (2009).
- [8] K. Inoue, H. Oda, A. Yamanaka, N. Ikeda, H. Kawashima, Y. Sugimoto, and K. Asakawa, *Phys. Rev. A* **78**, 011805(R) (2008).
- [9] J. F. McMillan, M. B. Yu, D. L. Kwong, and C. W. Wong, *Appl. Phys. Lett.* **93**, 251105 (2008).
- [10] X. Checoury, M. El Kurdi, Z. Han, and P. Boucaud, *Opt. Express* **17**, 3500 (2009).
- [11] R. W. Boyd, *Nonlinear Optics* (Academic Press, New York, 1992).
- [12] G. Bjork and Y. Yamamoto, *IEEE J. Quantum Electron.* **27**, 2386 (1991).
- [13] Q. Lin, O. J. Painter, and G. P. Agrawal, *Opt. Express* **15**, 16604 (2007).
- [14] M. El Kurdi, X. Checoury, S. David, T. P. Ngo, N. Zerounian, P. Boucaud, O. Kermarrec, Y. Campidelli, and D. Bensahel, *Opt. Express* **16**, 8780 (2008).

- [15] O. Boyraz and B. Jalali, *Opt. Express* **12**, 5269 (2004).
- [16] H. S. Rong, R. Jones, A. S. Liu, O. Cohen, D. Hak, A. Fang, and M. Paniccia, *Nature* **433**, 725 (2005).
- [17] J. I. Dadap, R. L. Espinola, R. M. Osgood, S. J. McNab, and Y. A. Vlasov, *Opt. Lett.* **29**, 2755 (2004).
- [18] M. Fujita, S. Takahashi, Y. Tanaka, T. Asano, and S. Noda, *Science* **308**, 1296 (2005).
- [19] X. D. Yang and C. W. Wong, *Opt. Express* **15**, 4763 (2007).
- [20] T. J. Kippenberg, S. A. Spillane, B. Min, and K. J. Vahala, *IEEE J. Sel. Top. Quant.* **10**, 1219 (2004).